Journal of Magnetism and Magnetic Materials 405 (2016) 107–116

Contents lists available at ScienceDirect

Journal of Magnetism and Magnetic Materials

journal homepage: www.elsevier.com/locate/jmmm

Electronic structure and magnetic properties of dilute U impurities in metals

S.K. Mohanta [a,*], S. Cottenier [b], S.N. Mishra [a]

[a] Tata Institute of Fundamental Research, Homi Bhabha Road, Mumbai-400005, India
[b] Center for Molecular Modeling, Ghent University, Technologiepark 903, 9053 Zwijnaarde, Belgium

ARTICLE INFO

Article history:
Received 10 November 2015
Received in revised form
9 December 2015
Accepted 12 December 2015
Available online 15 December 2015

Keywords:
Local magnetic moment
Ab initio calculation
5*f* impurity

ABSTRACT

The electronic structure and magnetic moment of dilute U impurity in metallic hosts have been calculated from first principles. The calculations have been performed within local density approximation of the density functional theory using Augmented plane wave+local orbital (APW+lo) technique, taking account of spin–orbit coupling and Coulomb correlation through LDA+U approach. We present here our results for the local density of states, magnetic moment and hyperfine field calculated for an isolated U impurity embedded in hosts with *sp*-, *d*- and *f*-type conduction electrons. The results of our systematic study provide a comprehensive insight on the pressure dependence of 5*f* local magnetism in metallic systems. The unpolarized local density of states (LDOS), analyzed within the frame work of Stoner model suggest the occurrence of local moment for U in *sp*-elements, noble metals and *f*-block hosts like La, Ce, Lu and Th. In contrast, U is predicted to be nonmagnetic in most transition metal hosts except in Sc, Ti, Y, Zr, and Hf consistent with the results obtained from spin polarized calculation. The spin and orbital magnetic moments of U computed within the frame of LDA+U formalism show a scaling behavior with lattice compression. We have also computed the spin and orbital hyperfine fields and a detail analysis has been carried out. The host dependent trends for the magnetic moment, hyperfine field and 5*f* occupation reflect pressure induced change of electronic structure with U valency changing from 3^+ to 4^+ under lattice compression. In addition, we have made a detailed analysis of the impurity induced host spin polarization suggesting qualitatively different roles of *f*-band electrons on moment stability. The results presented in this work would be helpful towards understanding magnetism and spin fluctuation in U based alloys.

1. Introduction

Studies of the local electronic structure and magnetism of dilute impurities in metallic hosts form a mainstream in the investigation of magnetism. Especially, electronic structure calculations have played an important role in providing the basis for understanding the underlying mechanism in a more concrete way. In this regard, *ab initio* calculations based on density functional theory (DFT) have been quite successful in providing a basis for understanding various physical properties of solids. Many different methods developed over the years have been applied to dilute alloys of *d* and *f* impurities, successfully reproducing the experimental results observed for magnetic moment as well as hyperfine fields [1–21]. While, extensive experimental and theoretical studies have been carried out for 3*d*, 4*d* and 4*f* impurities [22–26], very little is known on the electronic structure and magnetism of dilute 5*f* impurities in metallic hosts.

It is well established that 3*d* and 4*d* impurities in metallic hosts show qualitatively different types of magnetism as compared to 4*f* impurities. While, 3*d* and 4*d* electrons forming broad energy bands are treated to be itinerant and their magnetic behavior is often described by an effective spin S_{eff}, most of the 4*f* impurities exhibit Hund's rule moment corresponding to the LS coupled ground state of a well defined ionic ground state. On the other hand, the 5*f* wave function of the actinides are more extended compared to 4*f* electrons and strongly hybridize with the ligand states resulting broad *f*-band near the Fermi energy. Depending on the strength of hybridization, the 5*f* electrons of actinides are often treated as being localized or itinerant. The interplay of localization and itinerant (delocalized) behavior of 5*f* electrons have given rise to many exotic phenomena like heavy fermion, non-Fermi liquid and quantum critical behavior, especially in U based alloys. In this context, a number of studies have been carried out in many U based inter-metallic alloys [22,27–34] to elucidate localization/delocalization of 5*f* electrons. Investigations of electronic structure and magnetism for dilute alloys with actinide impurities are useful to understand moment formation and the interaction of 5*f*

* Corresponding author.

http://dx.doi.org/10.1016/j.jmmm.2015.12.042
0304-8853/

electrons with different types of host conduction electrons. While, experimental studies for dilute actinide alloys are few because of limited solubility, theoretical investigations are practically non-existent. Such studies are necessary not only to understand the formation of local moment on 5*f* impurities in metallic hosts but also to examine the interplay of localization and delocalization of 5*f* electrons. To this end we have carried out systematic theoretical calculations for dilute U impurities in different metallic hosts. Here, we present our results for the electronic structure and magnetic moment of dilute alloys of U in *sp*, *d* and *f* band metals allowing a comprehensive understanding of moment formation and the influence of different types of host conduction electrons on the spin and orbital magnetism of the impurity atom. Based on Stoner analysis of the local density of states, we find that local moment formation is supported for U in most of the *sp*-metals including Cu, Ag and Au. On the other hand, U in *d*-band metals is predicted to be magnetic only in the early transition metals viz. Sc, Ti, Y, Zr, La, Th and Ce while, in all other transition metal hosts (V–Ni); (Nb–Pd) and (Ta–Pt) U is found to be nonmagnetic. The host dependent variation of the calculated magnetic moment, occupation number and hyperfine field reflect lattice compression induced change in the electronic structure of U with valency changing from 3^+ to 4^+. The large 5*f* band width combined with the observation of high orbital moment supports interplay of itinerant and localized behavior for U-5*f* electrons.

2. Computational details

The calculations presented in this paper have been performed within the framework of density functional theory [35–37], using the augmented plane wave+local orbital (APW+lo) method [37–39] as implemented in the WIEN2k package [40] to solve the Kohn–Sham equation [36]. In order to study the electronic structure of the U impurity a supercell of dimension $2\times2\times2$ of the basic unit cell was constructed using experimental lattice parameters [41]. The supercell with one of the host atoms substituted by U represents a dilute alloy with impurity concentration of 1/16 at%. For a few representative cases (Sc, Ti, Zn, In) calculations were also performed with a larger supercell ($3\times3\times3$) to examine possible impurity–impurity interaction. The inter-impurity distance in the supercells used for our calculations are large enough to ignore the effect of impurity–impurity interaction. In the APW+lo method, the unit cell is divided into two regions: (i) non-overlapping muffin-tin sphere of radius R_{MT} and (ii) remaining the so-called interstitial region. The wave functions within the atomic spheres are expanded in spherical harmonics and plane waves are used for the interstitial region. In our calculations we have used R_{MT}=2.1–2.4 a.u. for the host metals and 2.8 a.u. for U. The maximum multipolarity l of the wave function within the atomic sphere was restricted to l_{max}=10. The wave functions in the interstitial region were expanded as plane waves with a cutoff wave vector $K_{max}=7.5/R_{MT}^{min}=3.571$. The charge density was Fourier expanded up to $G_{max}=16\sqrt{Ry}$. For the exchange and correlation we have used the gradient corrected local density approximation (GGA) [42]. For sampling the Brillouin zone a dense *k*-mesh of size $10\times10\times10$ was used. For each of the cases lattice relaxation was adopted to minimize the force on each atom to less than 1 mRy/a.u. The self-consistency of the calculations are ascertained from the charge and energy convergence criterion set to be 0.0001 and 0.01 mRy respectively.

The spin and orbital contributions to the magnetic moment and hyperfine fields were extracted from spin polarized calculations using LSDA+U method taking account of the spin–orbit interaction and onsite Coulomb correlation, applying two schemes: (i) orbital polarization (OP) method developed by Brooks et al. [43,44] and (ii) mean field formalism of Anisimov et al. [45,46]. In OP method the Coulomb parameter U and the exchange integral J entering the energy functional are calculated self-consistently. This parameter free technique has been found to work well for *f*-electron systems as well as in strongly localized d ions e.g. Fe in alkali metal hosts [5,6,44,47,48]. However, in several other cases, especially in strongly correlated electron systems involving 4*f* and 5*f* electrons the OP method has been found to over estimates the orbital magnetic moment and the corresponding hyperfine field. The mean field approach on the other hand has been found to be successful in many cases. In this case the effective Coulomb energy $U_{eff}=U-J$ enters the energy functional as an external parameters. For our cases, we have taken U_{eff}=0.20 Ry consistent with the values reported from X-ray photo-emission (XPS) and Bremsstrahlung isochromat spectroscopy (BIS) measurements as well as recent theoretical calculations [49–51]. The spin and orbital moments as well as the hyperfine fields obtained from these calculations were found to be similar within accuracy limit.

Here we would like to note that because of the limitations of the LDA+U schemes adopted for our calculations, especially the different treatments of the onsite Columb interaction U_{eff} the calculated orbital magnetic moment may differ in magnitude. However, as will be discussed later, the uncertainty in U_{eff} does not alter the general trends observed for the magnetic moment and hyperfine fields which is the main focus of this study. We also like to add that in recent years several new methods have been developed to overcome the limitations of standard LDA+U approach to get more realistic description of correlated electron systems [52–54]. In particular, density functional theory combined with dynamic mean field theory (DFT+DMFT) have been found to be quite successful in providing improved understanding of band structure in strongly correlated 5*f* electron systems, especially Pu metal and its alloys [55,56]. To our knowledge DFT+DMFT method has not been applied extensively to study magnetism of dilute 5*f* impurities in metallic hosts except the case of Pu in Th [56]. A detailed study of 5*f* impurity magnetism in metallic hosts using DFT+DMFT method is beyond the scope of this work.

3. Results and discussion

Let us first discuss the results of the nonmagnetic (without spin polarization) calculations and examine the host dependent moment formation for U impurity. Formation of local moment on an impurity atom is governed by Stoner criterion $IN_l(E_F)>1$, where I is the Stoner parameter and $N_l(E_F)$ is the nonmagnetic local density of states at Fermi energy E_F for the impurity atom. Fig. 1 shows the projected local density of states (DOS) for U in different hosts. It can be noticed that in most of the *sp*-band hosts the U-5*f* DOS show a narrow peak near the Fermi energy reflecting the formation of a virtual bound state (VBS). In the case of *d*- and *f*-band metal hosts, the 5*f* VBS is observed for the early members of the series like Sc, Ti, Y, Zr, La, Th, Ce and Yb. The narrow 5*f*-width observed for most of the cases is consistent with weak crystal field splitting with magnitude $\lesssim$0.5 eV [57,58]. The host dependent change in the electronic configuration of U will be discussed in the later part of the paper. In most of the cases studied here except Ce and Yb, the U-5*f* VBS has little overlap with the host band electrons. For U in Ce and Yb, the impurity 5*f* VBS strongly overlaps with the host 4*f* band. Notice that with decreasing host volume i.e. lattice compression, the 5*f* peak of U become broader and shifts away from the Fermi energy. This is more clearly visible in transition metal hosts with 5*f* peak pushed above the Fermi energy for the hosts: V, Mo, Ru, Rh, Pd, Ta, W and Pt. The calculated U-5*f* local density of states at Fermi energy $N_l(E_F)$ are displayed in Fig. 2.

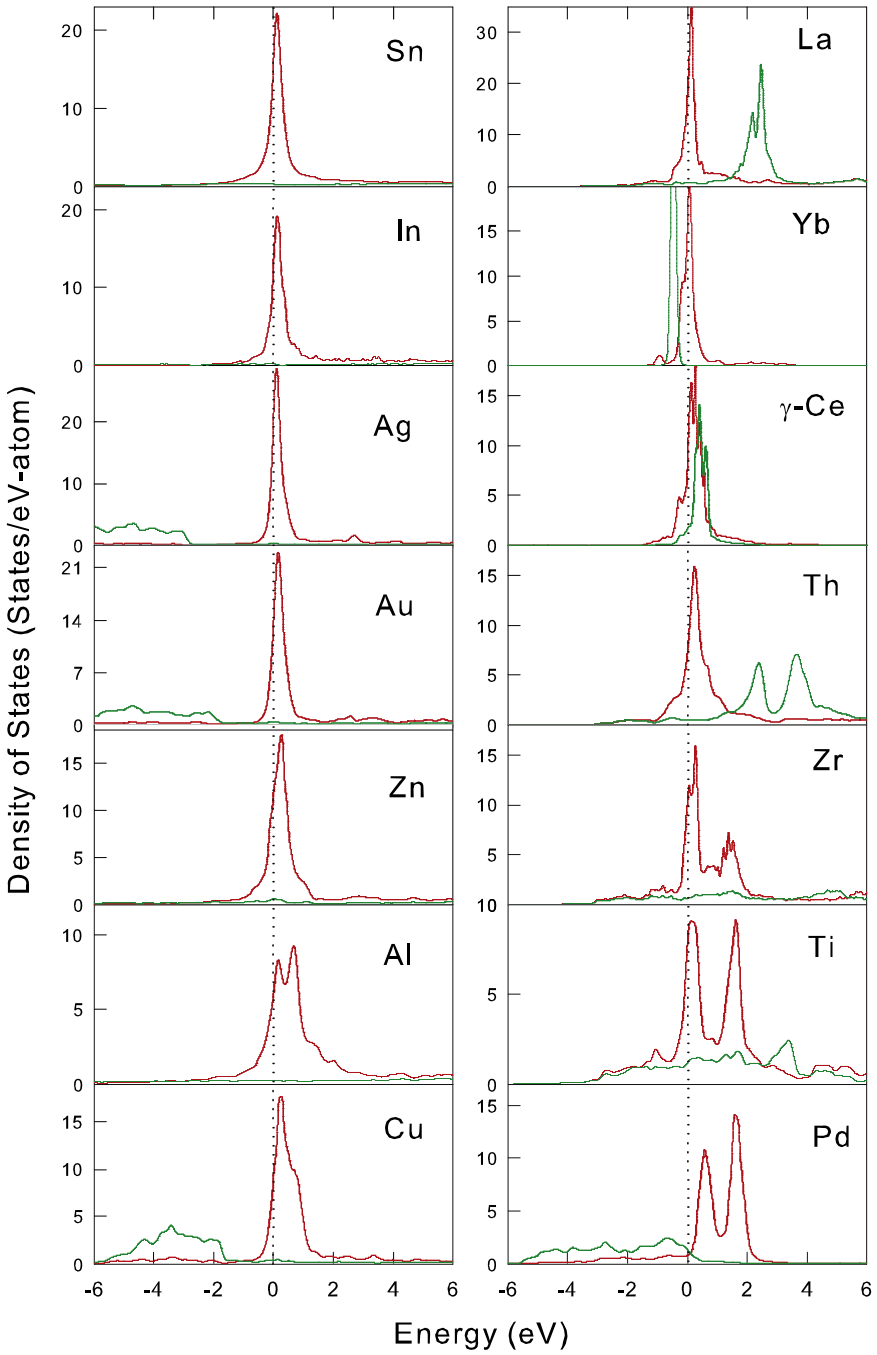

Fig. 1. Unpolarized density of states (DOS). Solid (red) lines correspond to U-5*f* and solid (green) lines represent host DOS. The dotted line represents Fermi level. (For interpretation of the references to color in this figure caption, the reader is referred to the web version of this paper.)

Using the $N_l(E_F)$ values obtained from our calculations and taking $I=0.25$ for U [44,59] we find that Stoner criterion for moment formation is satisfied for most of the *sp*-band metals including noble metal hosts. In the transition series, moment formation is supported for elements in the first two columns: Sc, Ti, Y, Zr and Hf. In all other *d*-band metals (V–Ni, Nb–Pd, Ta–Pt) U impurity is predicted to be nonmagnetic. Local moment formation is also supported for U in *f*-block elements La, Ce, Yb and Th. The predicted magnetic behavior of U in metallic hosts are consistent with the experimental results available for Au, Th and Pd hosts [28,29,32,33,60]. The magnetic behavior of U predicted from Stoner criterion is more clearly illustrated by results obtained from spin polarized calculations discussed below.

We now examine the spin polarized density of states and discuss the spin and orbital moments of the U impurity in different hosts. Fig. 3 displays the spin resolved local density of states (LDOS) for the U impurity in different host matrices. The U-5*f* bands are quite broad, resembling the features of itinerant *d*-electrons in transition metals and alloys. Consistent with the Stoner prediction discussed above the 5*f* spin bands of U show visibly large exchange splitting. With a decrease of the host volume (increasing lattice pressure) the centroid of the occupied majority U-5*f* band straddling the Fermi energy progressively moves closer to E_F while, the minority 5*f* band above E_F remains almost unchanged, resulting in a gradual decrease in the exchange splitting. The spin and orbital magnetic moments, μ_{spin}, μ_{orb} of the U impurity atom in different hosts obtained from orbital polarization (OP) and LDA+U (mean field) methods are summarized in

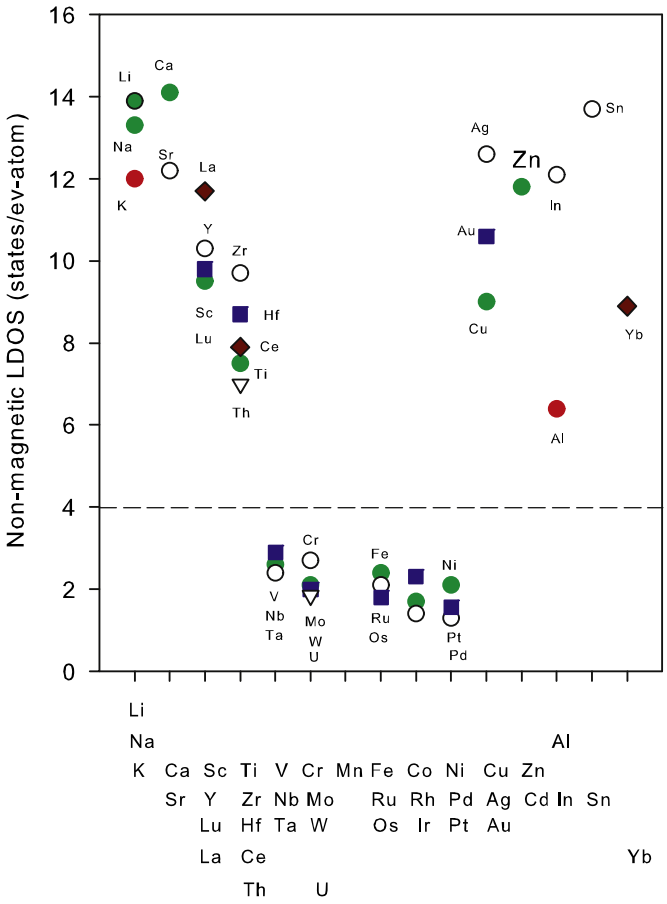

Fig. 2. U-5*f* local density of states at Fermi energy in different metallic hosts. Horizontal dotted line represents the Stoner limit for moment formation.

Table 1. It can be seen that U impurity in all the hosts, baring the transition metal hosts V–Ni; Nb–Pd and Ta–Pt show large spin and orbital moments. The moment values obtained from both OP and LDA+U (mean field) methods are close to each other and exhibit similar host dependent trends, which reassures that the results presented here illustrate the true lattice pressure dependence of U magnetism. From here on we discuss the host dependent changes in U magnetic behavior based on the results obtained from LDA+U calculations.

The spin and orbital moments of the U impurity atom in large volume hosts e.g. Na, Ca and Yb are found to be close to Hund's rule value of U ($5f^3$) configuration. On the other hand the magnetic moments of U in small volume hosts like Cu, Zn and Ti are found to be substantially small. Especially note worthy is the observation of high orbital moment on U. The existence of orbital moment provides crucial information regarding intra-atomic spin and orbital correlation – Hund's rule coupling. It is well recognized that orbital moments in itinerant *d*-electron systems are generally small because of weak spin–orbit (L–S) coupling and comparatively large crystal field (CF) splitting and/or hybridization. On the other hand, large orbital moments are observed for highly localized 4*f* electrons due to stronger L–S coupling and much weaker CF splitting [57,58]. Since 5*f* electrons in U are more delocalized than 4*f* but have stronger L–S coupling than transition metal ions and the crystal field are relatively weak compared to *d* ions, it is of interest to see how the orbital moment changes with lattice pressure. To examine the host dependent changes in the spin and orbital moments of U impurity we analyze our data within the frame work of Anderson model. According to Anderson model the magnetic behavior of the impurity atom is governed by the virtual bound state (VBS) whose width $\Delta = \pi|V_{kf}|^2 N(E_F)$ depends on the hybridization strength V_{kd} which can be scaled by the lattice pressure proportional to the inverse of the host Wigner–Seitz volume $1/V$ [23,61]. Thus, the impurity moment is expected to decrease with increasing hybridization $\propto 1/V$. Fig. 4 display the variation of U spin moment as a function of lattice pressure parametrized by $1/V$. It can be seen that both μ_{spin} and μ_{orb} diminish linearly with lattice compression, falling more rapidly in transition metals than in *sp*-band hosts. This shows that moment reduction due to f–d hybridization is much stronger than f–sp interaction. Furthermore, in transition metal hosts the spin and orbital moments of the U impurity concomitantly disappear at lattice pressures close to 100 GPa whereas, they persist well beyond 150 GPa in *sp*-metal hosts. The results suggest that Hund's rule coupling remains intact up to the critical pressure beyond which the 5*f* level of U become quite broad and moves above the Fermi level (see Fig. 1) leading to complete lose of magnetism.

For further investigation on the pressure dependence of the U magnetic moment we have carried out LDA+U calculations for U in Al, Au, La and Th for which the condition for external pressure was simulated through lattice compression. For each of the cases studied, the value of the applied pressure for a given lattice compression was derived from Birch–Murnaghan equation of state [62]. Fig. 5 (left panel) shows the unpolarized U-*f* density of states in Al, Au, La and Th with 0 and 20% lattice compression. It can be noticed that, with the application of external pressure the impurity virtual bound state becomes quite broad, which indicates strong delocalization of U-5*f* electrons. The variation of U spin and orbital moments as a function of external pressure is displayed in the right panel of Fig. 5. The results reveal that spin and orbital moment of U decrease simultaneously and vanish together at a critical pressure P_{cr} which were found to be 32 GPa, 51 GPa, 62 GPa and 114 GPa (extrapolated value) for Th, La, Al and Au hosts respectively. The results, together with the host dependent trends discussed above (see Fig. 4), indicate that Hund's rule coupling remains intact up to a critical pressure above which the L–S coupled magnetic moments completely vanish – a feature akin to the behavior of strongly localized electrons e.g. 4*f* electrons in rare-earths. At the same time the broad *f*-band, progressively increasing with pressure, suggests itinerant behavior of the U-5*f* electrons. These two factors together demonstrate strong interplay of itinerant and localized behavior of U-5*f* electrons.

As noted before, in LDA+U approach the effective Coulomb energy enters the energy functional as an adjustable external parameter. Therefore, before discussing the results further it is pertinent to examine to what extent the moment values depend on U_{eff}. To this end we carried out the calculations for U in a few select hosts e.g. Au, Al, Th and Ti with different values of U_{eff} in the range 0–0.4 Ry. The calculated spin and orbital moments of U as a function of U_{eff} are displayed in Fig. 6. It can be noticed that the μ_{orb} and μ_{spin} values show an initial rise and levels off beyond $U_{\rm eff} = 0.15$ Ry. This is close to the value used in earlier calculations for U based systems [50,51,56].

The observed pressure dependence of U magnetism can be reconciled as being due to increasing Kondo interaction caused by progressive delocalization of *f*-electrons. Within Kondo model the impurity magnetic moment, in general, induces negative spin polarization of the host conduction band electrons giving rise to an antiferromagnetic exchange interaction causing moment instability below a characteristic Kondo temperature $T_K \propto \exp(-1/J\rho)$ [23]. Here, ρ is the density of states at Fermi energy E_F and J is the exchange interaction between the impurity moment and the conduction electrons. To examine the host dependence of the Kondo interaction we analyze the magnetic moment on the host atoms surrounding the impurity. The magnitude of the host spin polarization, largest for the first near neighbor,

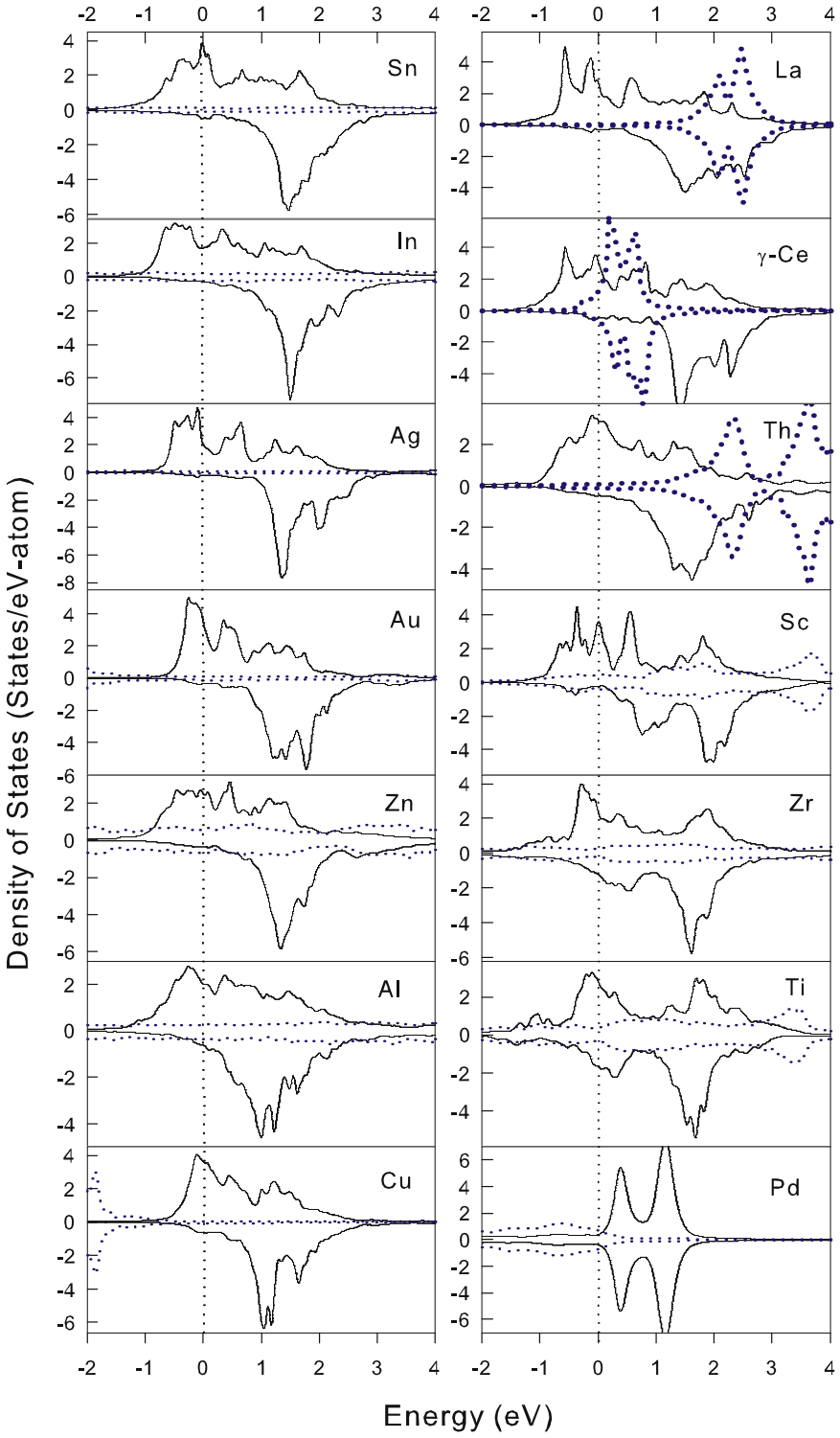

Fig. 3. Spin polarized local density of states (LDOS) of U-5*f* band (solid lines) in different hosts. Dotted lines represent the LDOS of first near neighbor host atom. For La, Ce and Th, the host LDOS correspond to 5*f* state.

rapidly decreases with increasing distance from the central impurity atom. The calculated induced spin moment for the host atoms in the first and second near neighbor shell of the impurity, m1 and m2 respectively, are listed in Table 1. It can be noticed that m1 and m2 values are small and negative for most of the *sp*-metal hosts. The induced moment on more distant near neighbors were found to be negligibly small. Baring the case of U in Ce (both γ and α phases) and Yb, the results for all other hosts reflect Kondo type antiferromagnetic exchange interaction between the impurity moment and host conduction band electrons which increases with decreasing Wigner–Seitz volume i.e. increasing lattice pressure. For the case of U in transition metal hosts the negative host spin polarization are found to be higher, consistent with increased overlap between U-*f* and host *d* band electrons. The enhanced antiferromagnetic exchange interaction at higher lattice pressure would lead to an increase in the T_K values and hence diminished magnetic response. The observed host dependence of U moment in *sp*- and *d*-band metals are consistent with Kondo model. They

Table 1
Summary of calculated magnetic properties of U impurity in different hosts obtained from orbital polarization (OP) and LDA+U (mean field) methods. The second column shows the Wigner–Seitz volume V_{WS} of the host. μ^{orb}, μ^{spin} are orbital, spin, and total magnetic moments from 5*f* electrons of the U impurity atom in units of Bohr magnetron (μ_B). m1 and m2 are the induced moments on near and next near neighbor host atoms, respectively.

Hosts	V_{WS} (Å^3)	OP				LDA+U			
		μ^{orb}	μ^{spin}	m1	m2	μ^{orb}	μ^{spin}	m1	m2
Ca	25.64	−5.24	2.73	−0.03	−0.008	−5.08	2.67	−0.03	−0.006
Na	23.81	−5.14	2.63	−0.04	−0.009	−4.97	2.48	−0.04	−0.007
Sn	16.13	−4.74	2.36	−0.05	−0.006	−4.62	2.29	−0.04	−0.006
In	15.63	−4.63	2.50	−0.03	−0.005	−4.51	2.35	−0.03	−0.004
Li	13.16	−4.66	2.41	−0.06	−0.013	−4.58	2.47	−0.06	−0.01
Ag	10.31	−4.28	2.27	−0.07	−0.020	−4.09	2.40	−0.08	−0.02
Au	10.20	−4.16	2.20	−0.08	−0.028	−3.95	2.08	−0.07	−0.02
Al	10.00	−3.73	1.84	−0.13	−0.034	−3.59	1.71	−0.11	−0.04
Zn	9.17	−3.56	1.72	−0.12	−0.029	−3.40	1.59	−0.10	−0.03
Cu	7.09	−2.90	1.27	−0.14	−0.044	−2.81	1.16	−0.12	−0.04
Y	19.23	−4.28	2.11	−0.07	−0.016	−4.10	2.24	−0.07	−0.03
Sc	14.93	−3.29	1.71	−0.05	−0.012	−3.13	1.80	−0.05	−0.02
Zr	14.08	−3.03	1.53	−0.04	−0.015	−2.88	1.36	−0.03	−0.01
Ti	10.64	−1.76	1.26	−0.17	−0.051	−1.59	1.07	−0.16	−0.05
Mo	9.43	0	0	0	0	0	0	0	0
Pd	8.85	0	0	0	0	0	0	0	0
V	8.33	0	0	0	0	0	0	0	0
Rh	8.26	0	0	0	0	0	0	0	0
Yb	26.34	−4.97	2.48	0.13	0.05	−4.89	2.34	0.13	0.05
La	22.73	−4.46	2.24	−0.07	−0.025	−4.67	2.15	−0.08	−0.03
$\gamma-Ce$	20.83	−4.41	2.20	0.31	0.14	−4.12	1.98	0.31	0.14
$\alpha-Ce$	17.29	−3.37	1.72	0.12	0.05	−3.18	1.63	0.12	0.04
Th	19.61	−4.20	2.16	−0.11	−0.04	−4.06	2.30	−0.13	−0.05
Lu	17.86	−4.01	2.03	−0.06	−0.01	−3.87	1.89	−0.07	−0.01

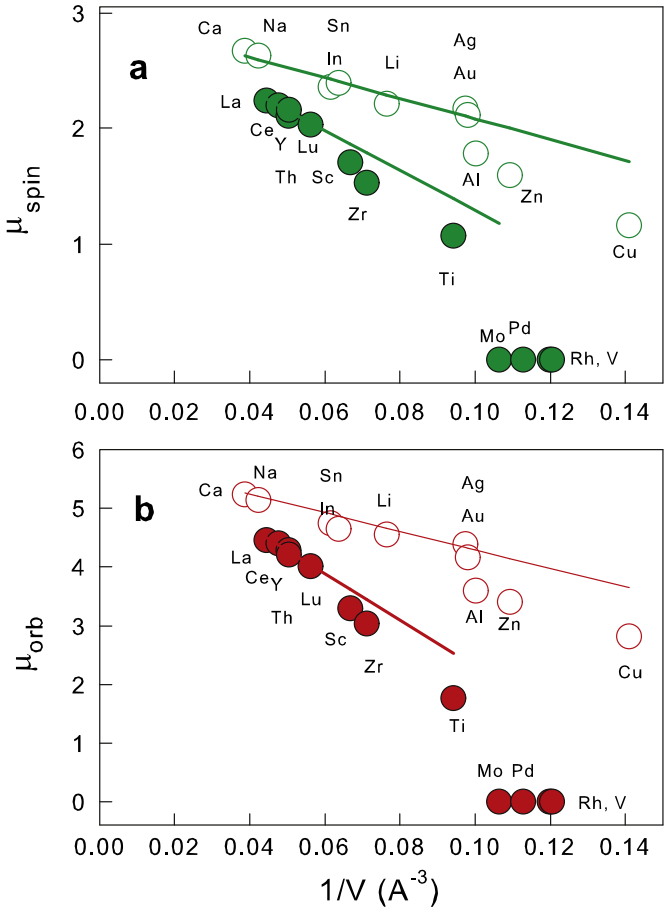

Fig. 4. (a) Spin and (b) orbital magnetic moment of U impurity in *sp*- (open circle) and *d*-band (filled circle) hosts. Lines represent a linear fit to the data points.

also agree with experimental trends observed from the pressure dependence of *d* and *f* moments in metallic hosts [63]. Moving to the *f*-band hosts, the host spin polarization in La, Th and Lu with unoccupied *f*-band come out to be significantly high and negative, suggesting stronger Kondo interaction, in agreement with the experimental observations [33]. In contrast, the host spin polarization for U in Ce and Yb are observed to be qualitatively different, being positive with sizable magnitude of $m1 = 0.24\,\mu_B$ and $m2 = 0.08\,\mu_B$ in γ-Ce. The results for U in α-Ce and Yb also show similar features. The positive host spin polarization observed for U in Ce and Yb bears striking similarity with the features observed for 3*d* impurities in Pd [64,65]. Looking at the LDOS results displayed in Fig. 2 it becomes clear that high spin polarization of host conduction band electrons in Ce and Yb arise mainly due to strong *f*–*f* interaction between U-5*f* and Ce-4*f* (Yb-4*f*) electrons. This can lead to intra-atomic ferromagnetic *f*–*f* exchange interaction over and above the usual antiferromagnetic interaction from *sp*-, *d*-band electrons which can lower the effective Kondo interaction strength and cause higher moment stability. Moment stabilizing influence of ferromagnetic host spin polarization has been earlier reported for 3*d*, 4*d* and 4*f* impurity atoms [24–26,66–68]. The results presented here show that the physical picture is more general and holds for all dilute moments including 5*f* impurities.

Coming to the possible change in the electronic structure of the impurity atom due to lattice compression, we have analyzed the orbital occupation for U in different hosts. The occupation of different orbitals within the atomic sphere of the U impurity obtained from the self-consistent solutions are displayed in Fig. 7. Starting from a nearly $5f^3$ (trivalent) configuration in large volume hosts like Ca, Na, La, the 5*f* occupation of U systematically decreases with lattice compression. Concomitantly, the *s* and *d* counts steadily increase with lattice pressure. Since, the APW+lo method uses non-overlapping atomic spheres, the occupation numbers obtained from the self-consistent solutions do not

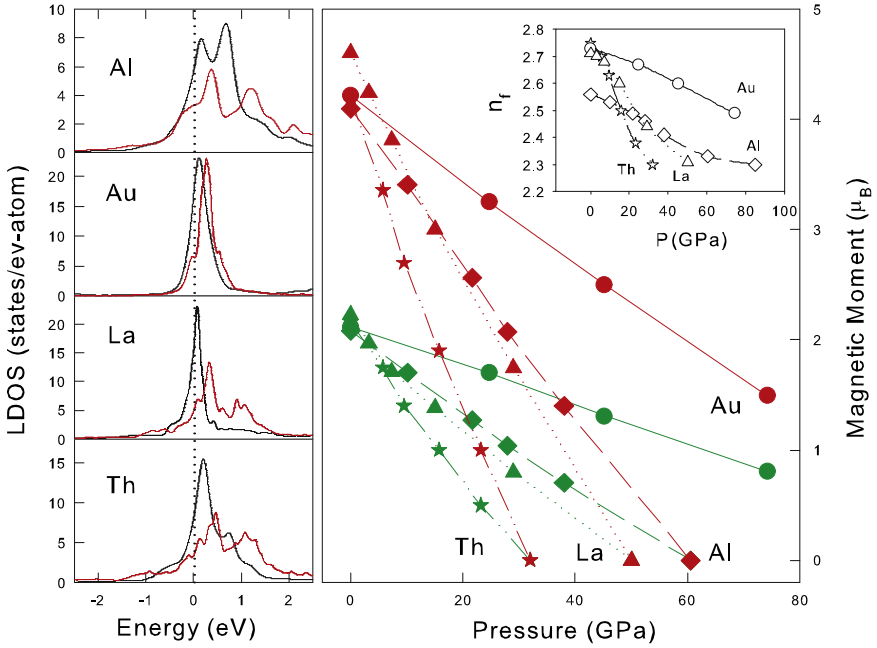

Fig. 5. (a) LDOS of U in Al, Au, La and Th under normal (black) and 20% lattice compression (red); (b) Pressure dependence of U spin (green) and orbital (red) moment in Al (⋄), Au (○), La (△) and Th (⋆).Inset shows the variation of 5*f* occupation as a function of pressure. (For interpretation of the references to color in this figure caption, the reader is referred to the web version of this paper.)

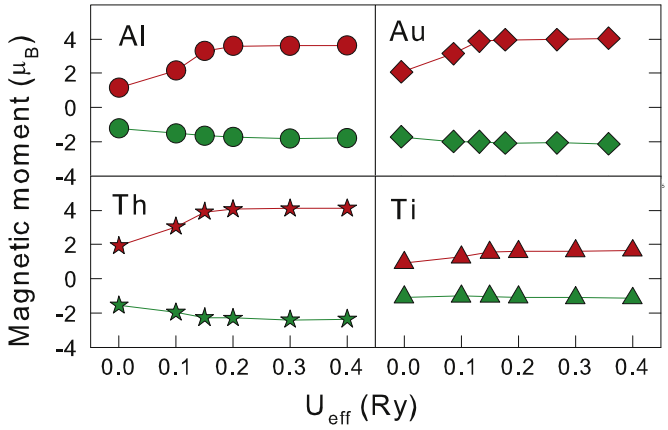

Fig. 6. Spin (green symbols) and orbital (red symbols) magnetic moment of U impurity in Au, Al, Th and Ti as a function of effective Coulomb repulsion parameter U_{eff} used in LDA+U calculations. (For interpretation of the references to color in this figure caption, the reader is referred to the web version of this paper.)

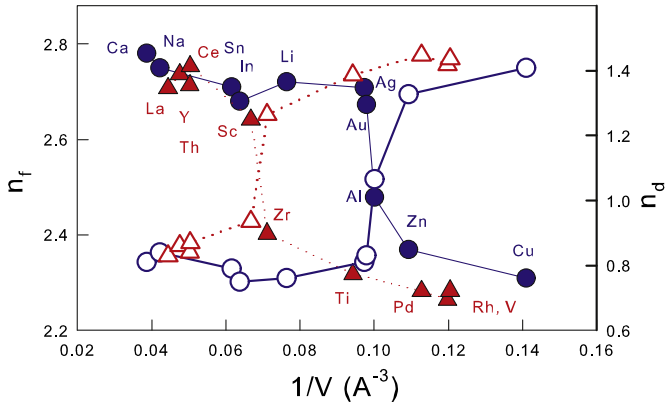

Fig. 7. Orbital occupation of U impurity in different hosts. Filled and open circles represent *f* and *d* occupation for U in *sp*-band metals. Filled and open triangles correspond to *f* and *d* occupation for U in transition metal hosts, respectively.

represent the true Mulliken population of the orbitals. The results, however, provide the qualitative trend for the redistribution of electrons in different orbitals. The results shown in Fig. 7 clearly reveal a change of the U valency, going from nearly trivalent (f^3) to tetravalent (f^2) configuration as the lattice pressure is increased.

It is important to compare the calculated results with available experiment data. As far as we know experimental measurements for dilute alloys with U impurity have been performed only for Au, Th and Pd hosts. The magnetic moment derived from the high temperature Curie–Weiss susceptibility indicated $5f^3$ behavior of U in Au and Th while a nonmagnetic behavior was reported for U in Pd [28,29,32,33,60]. Our calculated electronic structure of U in Au, Th and Pd are consistent with the experimental results, although the magnitude of the total magnetic moment is some what smaller. The discrepancy may be related to the fact that DFT calculations represent the behavior of U at zero temperature while, the experiments reported the effective moment derived from high temperature measurements. Nevertheless, it is gratifying to note that the features observed in our calculations, particularly the pressure dependence of the magnetic moment are in agreement with the trends reported from experimental measurements reported for a large number of U based intermetallic alloys [23,30,31].

We now come to discuss the magnetic hyperfine fields of U impurity in different hosts which provide useful microscopic information regarding its electronic structure and magnetic behavior. The spin (Fermi-contact) and orbital contributions to the magnetic hyperfine field, B_{hf}^{spin} and B_{hf}^{orb} respectively, were computed from the OP and LSDA+U calculations using prescriptions implemented within the WIEN2k code. The hyperfine fields calculated from the two techniques are summarized in Table 2. The host dependent variation of the hyperfine field components as a function of lattice pressure parametrized by inverse host volume are displayed in Fig. 8. Notice that the hyperfine fields show a step like transition at lattice compression corresponding to $1/V \approx 0.1$, coinciding with the change in the orbital occupation data (see Fig. 7). The hyperfine fields especially the core and valence

Table 2
Summary of calculated hyperfine fields of U impurity in metallic hosts in units of kG obtained from OP and LDA+U methods. B_{hf}^{orb}, and B_{hf}^{spin} are the contributions from orbital, and spin moments, respectively. B_{hf}^{core} and B_{hf}^{val} are contributions to the Fermi contact spin hyperfine field from core and valence electrons, respectively. Lines provide visual guidance.

Hosts	OP				LDA+U			
	B_{hf}^{orb}	B_{hf}^{spin}	B_{hf}^{core}	B_{hf}^{val}	B_{hf}^{orb}	B_{hf}^{spin}	B_{hf}^{core}	B_{hf}^{val}
Ca	3880	−324	−1363	1039	3834	−315	−1336	1021
Na	3806	−319	−1349	1030	3785	−310	−1319	1009
Sn	3508	−293	−1281	988	3576	−285	−1251	966
In	3552	−285	−1274	989	3502	−279	−1216	937
Li	3466	−274	−1151	877	3484	−266	−1180	914
Ag	3371	−231	−1065	834	3319	−240	−1108	868
Au	3182	−218	−1037	819	3134	−206	−1057	851
Al	2859	−186	−930	744	2891	−169	−864	671
Zn	2595	−177	−851	674	2567	−175	−787	593
Cu	2161	−155	−789	634	2136	−146	−750	568
Y	3177	−256	−1082	826	3124	−256	−1125	869
Sc	2580	−240	−998	758	2506	−247	−1042	791
Zr	2139	−221	−944	723	2073	−218	−863	686
Ti	1682	−162	−861	699	1625	−162	−785	623
Mo	0	0	0	0	0	0	0	0
Pd	0	0	0	0	0	0	0	0
V	0	0	0	0	0	0	0	0
Rh	0	0	0	0	0	0	0	0
Yb	3513	−251	−1275	1024	3539	−251	−1203	1049
La	3203	−258	−1214	956	3235	−258	−1165	907
$\gamma-Ce$	3174	−252	−1269	1017	3141	−252	−1142	890
$\alpha-Ce$	2359	−202	−942	740	2390	−202	−893	691
Lu	2967	−247	−1021	774	2972	−247	−1087	840
Th	3040	−249	−1185	936	3005	−249	−1103	854

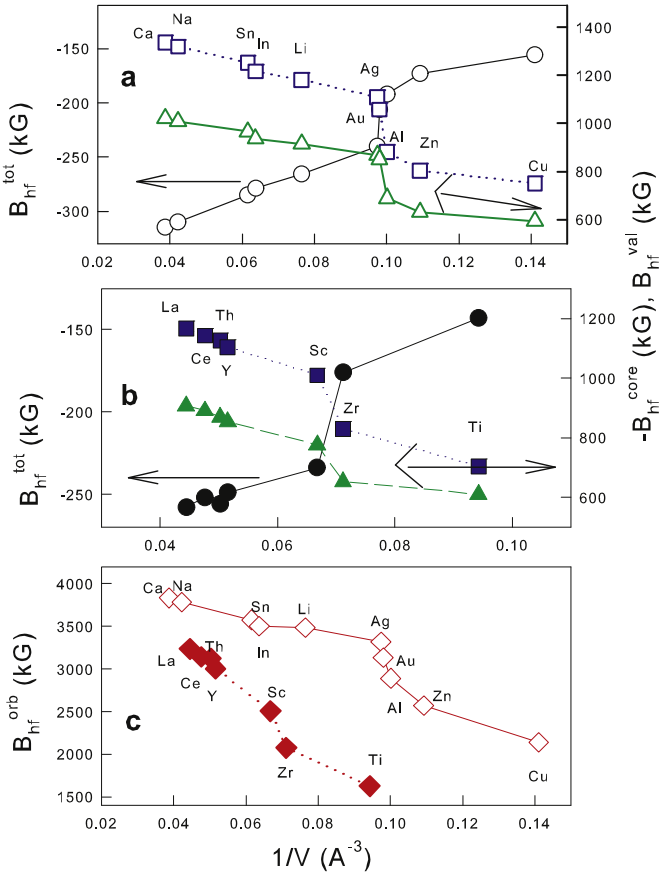

Fig. 8. Variation of hyperfine fields for U in different hosts as a function of inverse volume $1/V$: (a), and (b) correspond to Fermi contact and orbital hyperfine fields for U in *sp*- and *d*-band metals respectively. Square, triangle and circles correspond to contributions from core polarization B_{hf}^{core}, valence electrons B_{hf}^{val} and total $B_{hf}^{tot} = B_{hf}^{core} + B_{hf}^{val}$, respectively. Panel (c) represents the orbital hyperfine field of U in *sp*-metals (open symbol) and *d*-band hosts (filled symbols).

contributions to the Fermi contact field sharply change, reflecting a large change in the magnitude of the hyperfine coupling constant A due to delocalization of U-*f* electrons resulting in a cross-over of valency from 3^+ to 4^+. For further illustration of the host dependent change of electronic structure of U we look at the scaling behavior of the hyperfine fields. The orbital and spin hyperfine fields usually scale with the respective components of the magnetic moments of the impurity atom: $B_{hf} = A\mu$, where A is the hyperfine coupling constant [69,70]. Fig. 9 shows the plot of hyperfine fields against the spin or orbital moment of U calculated for different hosts. A linear fit of the data yield an average orbital hyperfine coupling constants A_{orb}=731 kG/μ_B for U in *sp*-metals and 593 kG/μ_B in *d*-band hosts. The estimated A_{orb} for U is significantly smaller than the values observed for 4*f* ions, but larger compared to the typical values found for 3*d* and 4*d* impurities [69,70]. This is consistent with the fact that 5*f* orbital of U is relatively more delocalized than 4*f* orbitals but more localized compared to *d* electrons. Coming to the Fermi contact (spin) hyperfine field, the hyperfine couplings for the core and valence contributions change with lattice compression yielding average value for $A_{core} \approx -626$ kG/μ_B and $A_{val} \approx 530$ kG/μ_B for *sp*-hosts. The corresponding values in the transition metal hosts were found to be −530 kG/μ_B and 417 kG/μ_B. The reduction in the Fermi contact fields in *d*-band metals as compared to *sp*-metal hosts are consistent with the trends for the hybridization of U-5*f* electrons yielding lower moment values. More importantly, a fit of the core and valence contributions to the hyperfine field yield $A_{core} = -226 \pm 24$ kG for large volume hosts Ca–Au. On the other hand a significantly lower value of $A_{core} = -143 \pm 11$ kG was found for U in small volume hosts Al, Zn and Cu. Similarly, the valence field coupling constant A_{val} was found to change from 360 ± 32 kG to 195 ± 17 kG. In the case of transition metal hosts the values for A_{core} and A_{val} were estimated to be −275 ± 20 kG and 233 ± 26 kG respectively for hosts La–Au. The corresponding values in small volume hosts Zr and Ti were found to be −126 ± 13 kG and 77 ± 14 kG. The reduction in the hyperfine field coupling constants at lattice compression equivalent to $1/V \sim 0.1$ are consistent with delocalization of *f*-electrons and corroborate the pressure induced change in the electronic structure of U discussed above.

Finally we discuss the influence of lattice relaxation on the magnetic moment and hyperfine field of U in different hosts. In the supercell approach adopted here, due to lattice imperfection caused by the presence of an impurity the atoms at their ideal positions experience non-zero force which must be minimized to obtain the ground state solution. This is achieved by allowing the atoms to move to new positions (lattice relaxation) and the self-consistency cycle was repeated until the force became below 1 mRy/a.u. In all the cases studied here, structural relaxation was applied to unpolarized as well as spin polarized calculations. For LDA+U calculations we have used the relaxed structure corresponding to the respective spin polarized cases. The self-consistent solutions corresponding to the fully relaxed atomic positions showed outward movement of the host atoms, the displacement being maximum for the first nearest neighbor (1 NN) shell and falling off rapidly with increasing distance from the central impurity. Fig. 10 displays the force and displacement of the 1 NN host atom with respect to the unrelaxed structure. The magnetic moments and hyperfine fields obtained from the self-consistent solution with and without lattice relaxation are summarized in

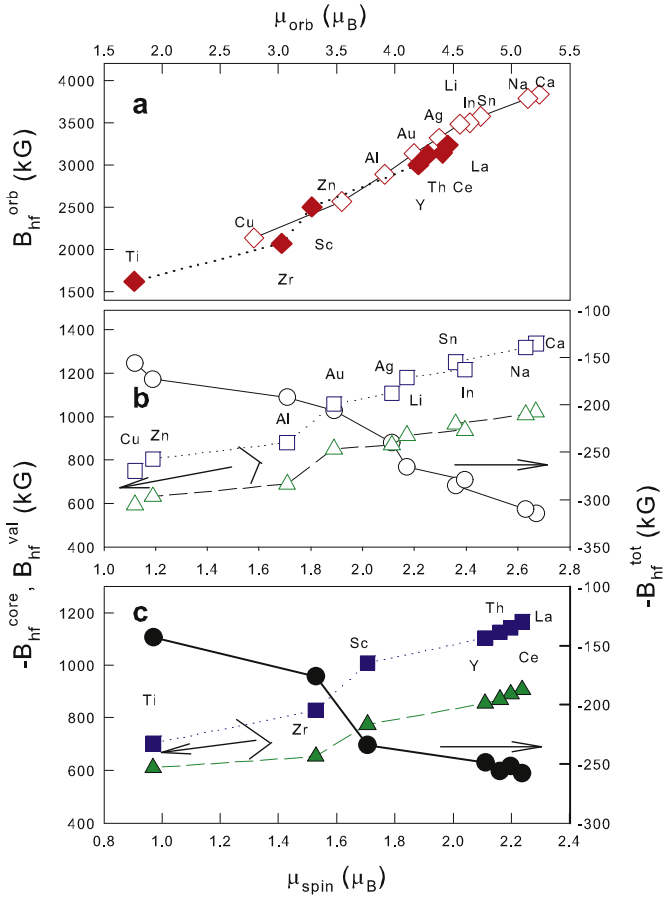

Fig. 9. Variation of hyperfine fields for U in different hosts as a function of impurity moment. Panel (a) corresponds to the orbital hyperfine field B_{hf}^{orb}. Panels (b) and (c) show the Fermi contact fields of U in *sp*- and *d*-band metals hosts respectively: square, triangle and circles correspond to contributions from core polarization B_{hf}^{core}, valence electrons B_{hf}^{val} and total $B_{hf}^{tot} = B_{hf}^{core} + B_{hf}^{val}$ hyperfine fields, respectively. Open and filled symbols correspond to *sp*- and *d*-band hosts respectively.

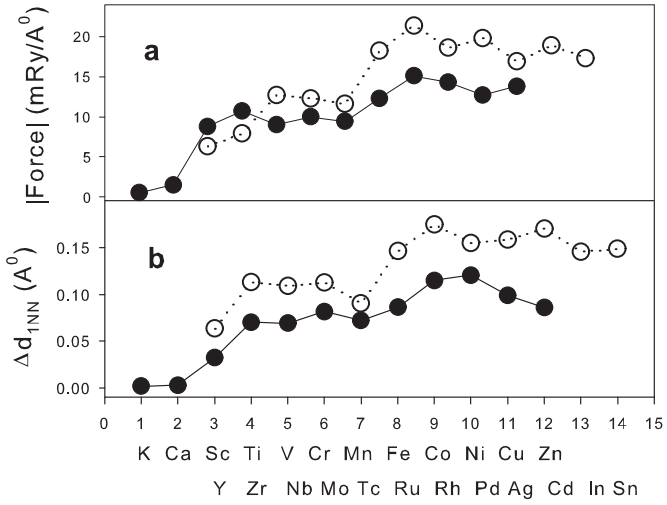

Fig. 10. (a) Force on nearest neighbor (1 NN) host atoms in an unrelaxed lattice and (b) displacement of 1 NN host atoms relative to the unrelaxed structure. Filled and open symbols correspond to hosts K–Zn and Y–Sn respectively.

Table 3. It can be noticed that the magnetic moment and hyperfine field of trivalent U in large volume hosts: Na, Li, Ca, Sn, In, Ag, Au, Yb, La, Y, Th, Lu marginally change after considering lattice relaxation. On the other hand, in small volume hosts like Al, Zn, Cu, Zr and Ti the μ and B_{hf} values of U significantly decrease in comparison to the unrelaxed cases. We like to emphasize that the observed change in magnetic moment and hyperfine field due to lattice relaxation does not alter the host dependent trends which is the main emphasis of this work. In all the cases studied here, structural relaxation was applied to unpolarized as well as spin polarized calculations until the force became below 1 mRy/a.u. For LDA+U calculations we have used the relaxed structure corresponding to the respective spin polarized cases. The self-consistent solutions corresponding to the fully relaxed atomic positions showed outward movement of the host atoms, the displacement being maximum for the 1 NN shell and falling off rapidly with increasing distance from the central impurity. Fig. 10 displays the force and displacement of the nearest neighbor host atom with respect to the unrelaxed structure. The magnetic moments and hyperfine fields obtained from the self-consistent solution with and without lattice relaxation are summarized in Table 3. It can be noticed that the magnetic moment and hyperfine field of trivalent U in large volume hosts: Na, Li, Ca, Sn, In, Ag, Au, Yb, La, Y, Th, Lu marginally change after considering lattice relaxation. On the other hand, in small volume hosts like Al, Zn, Cu, Zr and Ti the μ and B_{hf} values of U significantly decrease in comparison to the unrelaxed cases. We like to emphasize that the observed change in magnetic moment and hyperfine field due to lattice relaxation does not alter the host dependent trends which is the main emphasis of this work.

Table 3
Magnetic moment and hyperfine field (in kG) of U in different hosts before and after lattice relaxation.

Hosts	μ^{orb}		μ^{spin}		B_{hf}^{orb}		B_{hf}^{spin}	
	Unrel	Relax	Unrel	Relax	Unrel	Relax	Unrel	Relax
Ca	−5.01	−5.08	2.73	2.67	3820	3834	−321	−315
Na	−5.03	−4.97	2.77	2.48	3761	3785	−319	−310
Sn	−4.70	−4.62	2.36	2.29	3536	3576	−297	−285
In	−4.59	−4.51	2.40	2.35	3483	3502	−288	−279
Li	−4.63	−4.58	2.49	2.41	3468	3484	−280	−266
Ag	−4.13	−4.09	2.44	2.40	3301	3319	−224	−240
Au	−3.99	−3.95	2.12	2.08	3112	3134	−195	−206
Al	−3.54	−3.59	1.97	1.71	2824	2891	−178	−169
Zn	−3.29	−3.34	1.86	1.59	2514	2567	−153	−175
Cu	−2.45	−2.81	1.58	1.06	2090	2136	−118	−146
Y	−4.24	−4.10	2.17	2.24	3157	3124	−279	−256
Sc	−3.35	−3.13	1.94	1.80	2489	2506	−234	−247
Zr	−3.07	−2.88	1.62	1.36	2041	2073	−196	−218
Ti	−1.81	−1.59	1.39	0.97	1668	1625	−143	−162
Yb	−4.97	−4.89	2.42	2.34	3578	3539	−266	−251
La	−4.75	−4.67	2.23	2.15	3251	3235	−272	−258
$\gamma - Ce$	−4.26	−4.12	2.19	1.98	3160	3141	−269	−252
$\alpha - Ce$	−3.37	−3.18	1.75	1.63	2584	2390	−178	−202
Th	−4.15	−4.06	2.41	2.30	2990	2972	−261	−247
Lu	−4.01	−3.87	1.92	1.89	3031	3005	−258	−249

4. Summary

In summary, we have performed detailed electronic structure calculations for dilute U impurity embedded in metallic hosts. The results of our *ab initio* calculations performed within the LDA+U approach of the density functional theory allowed us to establish the host dependent trends for the local density of states, orbital occupation, magnetic moment and hyperfine field, together providing a comprehensive insight on the occurrence of 5*f* local moment and its pressure dependence. The results of our calculations demonstrate pressure induced localization–delocalization of 5*f* electrons with a clear signature of valence transition under lattice

compression. The pressure dependence of the U-5*f* band structure combined with the linear variation of the spin and orbital moments, concomitantly becoming zero above a characteristic host dependent critical pressure, illustrate the strong interplay between localized and itinerant behavior of U-5*f* electrons. In addition, we have made a detail analysis of the impurity induced host spin polarization and examined the sign and strength of exchange interaction of U-*f* moment with conduction electrons. The host spin polarization in *sp*- and *d*-band metals are found to be negative reflecting antiferromagnetic exchange coupling. In contrast, we find positive host polarization electrons in Ce and Yb hosts suggesting ferromagnetic interaction between U-*f* and host-*f* band electrons. Within Kondo model, we predict that the positive contribution to the exchange interaction from intra-atomic *f*–*f* exchange interaction can suppress spin fluctuation arising from negative *f*-*spd* exchange coupling and cause higher moment stability for the U impurity. The results presented in this work would be helpful towards understanding magnetism and spin fluctuation in U based alloys.

References

[1] V.S. Stepanyuk, R. Zeller, P.H. Dederichs, I. Mertig, Phys. Rev. B 49 (1994) 5157.
[2] N. Papanikolaou, N. Stefanou, R. Zeller, P.H. Dederichs, Phys. Rev. 46 (1992) 10858.
[3] M.E. McHenry, J.M. MacLaren, D.D. Vvedensky, M.E. Eberhart, M.L. Prueitt, Phys. Rev. 40 (1989) 10111.
[4] S.K. Kwon, B.I. Min, Phys. Rev. Lett. 84 (2000) 3970.
[5] G.Y. Guo, Phys. Rev. B 62 (2000) R14609.
[6] S. Frota-Pessoa, Phys. Rev. B 69 (2004) 104401.
[7] S. Blügel, H. Akai, R. Zeller, P.H. Dederichs, Phys. Rev. B 35 (1987) 3271.
[8] R. Zeller, J. Phys. F 17 (1987) 2123.
[9] B. Drittler, N. Stefanou, S. Blügel, R. Zeller, P.H. Dederichs, Phys. Rev. B 40 (1989) 8203.
[10] T. Beuerle, K. Hummler, C. Elsässer, M. Fähnle, R. Zeller, P.H. Dederichs, Phys. Rev. B 35 (1987) 3271.
[11] V.I. Anisimov, V.P. Antripov, A.J. Liechtenstein, V.A. Gubanov, A.V. Postnikov, Phys. Rev. B 37 (1988) 5598.
[12] G. Rahman, I.G. Kim, H.K.D.H. Bhadeshia, A.J. Freeman, Phys. Rev. B 81 (2010) 184423.
[13] S. Cottenier, H. Hass, Phys. Rev. B 62 (2000) 461.
[14] H. Akai, M. Akai, J. Kanamori, J. Phys. Soc. Jpn. 54 (1985) 4257.
[15] A.L. de Oliveira, M.V. Tovar Costa, N.A. de Oliveira, A. Troper, J. Magn. Magn. Mater. 320 (2008) e446–e449.
[16] W.D. Brewer, E. Wehmeier, Phys. Rev. B 12 (1975) 4608.
[17] W.D. Brewer, S. Hauf, D. Jones, S. Frota-Pessôa, J. Kapoor, Y. Li, A. Metz, D. Riegel, Phys. Rev. B 51 (1995) 12595.
[18] J. Boysen, J. Grimm, A. Kettschau, W.D. Brewer, G.V.H. Wilson, Phys. Rev. B 35 (1987) 1500.
[19] P. Leonard, N. Stefanou, J. Phys. 43 (1982) 1497.
[20] H. Akai, M. Akai, S. Blügel, R. Zeller, P.H. Dederichs, J. Magn. Magn. Mater. 45 (1984) 291.
[21] P.H. Dederichs, R. Zeller, H. Akai, S. Blügel, A. Oswald, Philos. Mag. B 51 (1985) 137.
[22] O. Madelung (Ed.), Landolt-börnstein, New Series III, vol. 19, Springer, Heidelberg, 1989.
[23] For a review see A.C. Hewson, The Kondo Problem to Heavy Fermion, Cambridge University Press, Cambridge, 1993.
[24] D. Riegel, L. Büermann, K.D. Gross, M. Luszik-Bhadra, S.N. Mishra, Phys. Rev. Lett. 62 (1989) 316.
[25] S. Khatua, S.N. Mishra, S.H. Devare, H.G. Devare, Phys. Rev. Lett. 68 (1992) 1038.
[26] A.A. Tulapurkar, S.N. Mishra, R.G. Pillay, H.G. Salunke, G.P. Das, S. Cottenier, Phys. Rev. Lett. 85 (2000) 1978.
[27] L. Petit, A. Svane, W.M. Temmerman, Z. Szotek, Phys. Rev. Lett. 88 (2002) 216403.
[28] F.U. Hillebrecht, H.J. Trodahl, V. Sechovsky, B.T. Thole, Z. Phys. B—Condens. Matter 77 (1989) 373–380.
[29] S. Tsutsui, M. Nayakada, Y. Kobayashi, S. Nasu, Y. Haga, Y. Onuki, Hyperfine Interact. 133 (2001) 17–21.
[30] J.M. Fournier, Physica 130B (1985) 268.
[31] G.R. Stewart, Rev. Mod. Phys. 73 (2001) 797.
[32] W.J. Nellis, M.B. Brodsky, H. Montgomery, G.P. Pells, Phys. Rev. B 2 (1970) 4590.
[33] M.B. Maple, J.G. Huber, B.R. Coles, A.C. Lawson, J. Low Temp. Phys. 3 (1970) 2.
[34] B.D. Dunlap, G.W. Crabtree, J.D. Jorgensen, H.A. Kierstead, D.D. Koelling, W. K. Kwok, D.J. Lam, S.K. Malik, A.W. Mitchell, S.C. Strite, Phys. Rev. B 39 (1989) 5640.
[35] P. Hohenberg, W. Kohn, Phys. Rev. 136 (1964) B864.
[36] W. Kohn, L.J. Sham, Phys. Rev. 140 (1965) A1133.
[37] S. Cottenier, Density Functional Theory and the family of (L)APW-methods: a step-by-stem introduction (Instituut voor Kern-en Stralingsfysica, K.U. Leuven, Belgium) (freely available at ⟨http://www.wien2k.at/reg_users/textbooks⟩).
[38] E. Sjöstedt, L. Nordström, D.J. Singh, Solid State Commun. 114 (2000) 15.
[39] G.K.H. Madsen, P. Blaha, K. Schwarz, E. Sjöstedt, L. Nordström, Phys. Rev. B 64 (2001) 195134.
[40] P. Blaha, K. Schwarz, G. Madsen, D. Kvasnicka, J. Lutiz, computer code wien2k, an augmented plane wave+local orbital program for calculating crystal properties, Karlheinz Schwarz, Technische Universität Wien, Austria, 1999.
[41] W.B. Pearson, A Handbook of Lattice Spacing and Structure of Metals and Alloys, vol. 2, Pergamon Press, London, 1967.
[42] J.P. Perdew, Y. Wang, Phys. Rev. B 45 (1992) 13244.
[43] M.S.S. Brooks, Physica B 130 (1985) 6.
[44] M.S.S. Brooks, O. Eriksson, B. Johansson, J.J.M. Franse, P.H. Frings, J. Phys. F: Met. Phys 18 (1988) L33.
[45] V.I. Anisimov, J. Zaanen, O.K. Andersen, Phys. Rev. B 44 (1991) 943.
[46] V.I. Anisimov, I.V. Solovyev, M.A. Korotin, M.T. Czyzyk, G.A. Sawatzky, Phys. Rev. B 48 (1993) 16929.
[47] O. Eriksson, M.S.S. Brooks, B. Johansson, Phys. Rev. B 41 (1990) 7311; O. Eriksson, B. Johansson, R.C. Albers, A.M. Boring, M.S.S. Brooks, Phys. Rev. B 42 (1990) 2707.
[48] P. Soderlind, P.E.A. Turchi, A. Landa, V. Lordi, J. Phys.: Condens. Matter 26 (2014) 416001.
[49] Y. Baer, H.R. Ott, K. Andres, Solid State Commun. 36 (1980) 387–391.
[50] A.N. Yaresko, V.N. Antonov, P. Fulde, Phys. Rev. B 67 (2003) 155103.
[51] W. Xie, W. Xiong, C.A. Marianetti, D. Morgan, Phys. Rev. B 88 (2013) 235128.
[52] I.V. Solovyev, A.I. Liechtenstein, K. Terakura, Phys. Rev. Lett. 80 (1998) 5758.
[53] I.V. Solovyev, Phys. Rev. Lett. 95 (2005) 267205.
[54] K.T. Moore, G. van der Laan, Rev. Mod. Phys. 81 (2009) 235.
[55] J.H. Shim, K. Haule, G. Kotliar, Nature 446 (2007) 05647.
[56] Jian-Xin Zhu, R.C. Albers, K. Haule, J.M. Wills, Phys. Rev. B 91 (2015) 165126.
[57] W.A. Hargreaves, Phys. Rev. B 2 (1970) 2273.
[58] W.T. Carnall, G.K. Liu, C.W. Williams, M.F. Reid, J. Chem. Phys. 95 (1991) 7194.
[59] O. Eriksson, B. Johansson, M.S.S. Brooks, H.L. Skriver, Phys. Rev. B 40 (1989) 9508.
[60] R.P. Guertin, J.B. Bulman, J.G. Huber, Physica B 102 (1980) 151–154.
[61] D. Van der Marel, G.A. Sawatzky, Phys. Rev. B 37 (1988) 10674.
[62] F.D. Murnaghan, Finite Deformation of an Elastic Solid, Wiley, New York, 1951.
[63] J.S. Schilling, Adv. Phys. 28 (1979) 657.
[64] J.F. van Acker, W. Speier, R. Zeller, Phys. Rev. B 43 (1991) 9558.
[65] V.S. Stepanyuk, W. Hergert, K. Wildberger, R. Zeller, P.H. Dederichs, Phys. Rev. B 53 (1996) 2121.
[66] S.K. Srivastava, S.N. Mishra, G.P. Das, J. Phys.: Condens. Matter 18 (2006) 9463–9470.
[67] V.V. Krishnamurthy, S.N. Mishra, M.R. Press, S.H. Devare, Phys. Rev. Lett. 74 (1995) 1661.
[68] S.N. Mishra, J. Phys.: Condens. Matter 15 (2003) 5333–5340.
[69] A.J. Freeman, in: A.J. Freeman, R.B. Frankel (Eds.), Hyperfine Interactions, Academic Press, New York, 1967 (chapter 2).
[70] B. Bleaney, in: R.J. Elliott (Ed.), Magnetic Properties of Rare Earth Metals, Plenum Press, New York, 1972 (chapter 8).